Polym. Bull. (2011) 67:343–360
DOI 10.1007/s00289-011-0464-5

ORIGINAL PAPER

Removal of heavy metals from aqueous solution by poly(acrylamide-co-acrylic acid) modified with porous materials

M. Zendehdel · A. Barati · H. Alikhani

Received: 4 December 2010 / Revised: 15 February 2011 / Accepted: 16 February 2011 /

Abstract In this study, a series of poly acrylamide-co-acrylic acid/NaY zeolite, poly acrylamide-co-acrylic acid/MCM-41, and poly acrylamide-co-acrylic acid/clinoptilolite nanocomposites were synthesized. These materials were characterized by using FT-IR spectroscopy, XRD, TGA, and SEM. Removal capacity of Pb(II) and Cd(II) ions in aqueous solutions by using these nanocomposites was investigated with controlled time, initial metal ions concentration, pH values, adsorbent content, and temperature by using atomic absorption spectrometry. Results show that these nanocomposites have further adsorption related to NaY, MCM-41, and clinoptilolite. Poly(AAm-co-AAc)/NaY, poly(AAm-co-AAc)/MCM-41, and poly(AAm-co-AAc)/clinoptilolite exhibit superior Pb(II) (about 90–99%) and Cd(II) (about 88–98%) adsorption behavior at room temperature and the poly(AAm-co-AAc)/NaY nanocomposite had the best adsorption behavior. Finally, the equilibrium removal performance of the composites is analyzed according to the Langmuir and Freundlich adsorption isotherm model that shows result fitted to Langmuir model and have monolayer adsorption.

Keywords Poly acrylamide-co-acrylic acid · Porous material · Removal · Pb(II) · Cd(II)

Introduction

Heavy metals are nowadays among the most important pollutants in source and treated water, and are becoming a severe public health problem, can be toxic to

M. Zendehdel (✉) · H. Alikhani
Department of Chemistry, Faculty of Science, Arak University, Arak, Iran
e-mail: m-zendehdel@araku.ac.ir; mojganzendehdel@yahoo.com

A. Barati
Department of Chemical Engineering, Faculty of Engineering, Arak University, Arak, Iran

aquatic life and cause natural waters to be unsuitable as potable water sources [1]. Lead is potentially toxic for humans via interaction with sulfhydryl group of proteins and aquatic lives causing reduction in root growth and loss of apical dominance of plants. In addition, adverse health effect due to cadmium has reported to cause renal disturbances, lung problems, bone lesions, cancer, and hypertension in humans. Then, removal of lead and cadmium from environments particularly from wastewater is very important [2–7]. In order to reduce heavy metal pollution problem, heavy metals in the environment removed by some processes such as oxidation–reduction processes, filtration, electrochemical treatment, evaporation, ion exchange or reverse osmosis, and adsorption [8].

Recently, the adsorption process with strong affinity and high loading capacity for targeted metal ions has developed much attention which has paid to modification of superabsorbent [9–11]. Superabsorbent hydrogels are loosely cross-linked hydrophilic polymers that can absorb, swell, and retain aqueous solutions up to hundred times their own weight. In the last several years, some attempts have been done to modify the properties of superabsorbents the incorporation of nano or micro particles of inorganic materials such as montmorillonite, kaolin, mica, bentonite, and sercite and laponite clay into polymer networks have been recently investigated [12–16]. Although, much preparation have focused on the improvement of the swelling ability, gel strength, mechanical and thermal stability of superabsorbents but adsorption of heavy metals by these composites is very important for selection of suitable adsorbent to metals removal from aqueous solutions [17–19].

In this study, a series of poly acrylamide-co-acrylic acid/NaY zeolite, poly acrylamide-co-acrylic acid/MCM-41, and poly acrylamide-co-acrylic acid]/clinoptilolite composites were synthesized and characterized. In addition, their removal capacity of Pb(II) and Cd(II) ions investigated in aqueous solutions. Finally, the equilibrium removal performance of the composites is analyzed according to the Langmuir and Freundlich adsorption isotherm model.

Experimental

Materials and methods

NaY zeolite with molar ratio: 16 NaOH:1 Al $(OH)_3$:15 SiO_2:320 H_2O [20] and MCM-41 with molar ratio: 1 TEOS:0.13 CTMABr:5.4 HCl:150 H_2O [21] were synthesized in our laboratory and activated according to the procedure described previously and all of them were used without further purification. Final product was characterized with X-Ray diffractometer (Philips 8440) with radiation at room temperature Cu K_α, FT-IR (Galaxy series FT-IR 5000 spectrometer), TGA (Diamond TG/DTA Perkin Elmer), and SEM (Philips, XL30).

Synthesis of poly(AAm-co-AAc)/NaY, MCM-41, clinoptilolite composites

The optimum molar ratio of initial materials for preparation of poly(AAm-co-AAc) considered at prior work in our laboratory [22]. Several nanocomposites were prepared with NaY zeolite, MCM-41, and clinoptilolite by radical graft copolymerization. Typical preparation conditions for samples are as follows:

At first, potassium acrylate was prepared by partially neutralizing a diluted acrylic acid solution with a predetermined amount of 50 wt% aqueous potassium hydroxide solution which was added drop wise in an ice bath. Then, the 0.23 g cross-linker (*N*,*N*′-methylene bis' acrylamide) carefully added to the acrylamide solution (3.19 g). Then, 0.2 g of NaY zeolite, MCM-41, or clinoptilolite that was ultrasounded for 1 h before use for getting nano size was slowly added to stirring monomer mixture. Then, the first neutralized solution was added to it. The obtained suspension was mixed by a 300-rpm magnetic mixer for 30 min. In the next step, TMED and APS (30 wt%) were added to the pore material–polymer mixed solution. Finally, the temperature of the reaction mixture was rapidly increased to 90 °C during less than 6 min. Then, the products removed from the beaker, cut to small pieces, and dried 72 to 96 h in laboratory conditions.

Adsorption studies

Adsorption experiments were evaluated in batch equilibrium mode. All experiments were done by mixing 25 mL of aqueous solution of Pb(II) and Cd(II) ions with different quantities (5, 10, 15, 20, and 25 mg) of synthetic composites. The mixtures were shaken in an orbital shaker (IKA-OS_2) at 300 rpm at desired temperature and contact time and then the suspensions were filtrated. The pH values of initial solutions were adjusted with 0.1 M HNO_3 or NaOH solution by using a (Metrohm-744) pH meter. For kinetic studies, 25 mg L^{-1} was chosen as the initial concentration of Pb(II) and Cd(II) solutions.

Adsorption experiments were also carried out to obtain isotherms at different temperature. This was done at 283, 293, 303, 313, and 323 K, respectively. In this study, Pb(II) and Cd(II) solutions with different initial concentration in the range of 50–2,000 mg L^{-1} were selected. Adsorption time of 120 min for Pb(II) and 60 min for Cd(II) was chosen to allow attainment of equilibrium at constant temperature.

The initial and final concentration of Pb(II) and Cd(II) in the aqueous solutions was measured with an atomic adsorption spectrophotometer. The percentage adsorption (%) was calculated by Eq. 1:

$$\%\ \text{Adsorption} = (C_\text{i} - C_\text{f})100/C_\text{i} \tag{1}$$

where C_i and C_f are the concentration of the metal ions in the initial and final solutions, respectively.

Results and discussion

FT-IR analysis

Figure 1a–d shows FT-IR spectra in the range of 500–4,000 cm^{-1} for the poly(AAm-co-AAc), poly(AAm-co-AAc)/NaY, poly(AAm-co-AAc)/clinoptilolite, and poly(AAm-co-AAc)/MCM-41, respectively. In Fig. 1a the broad band at

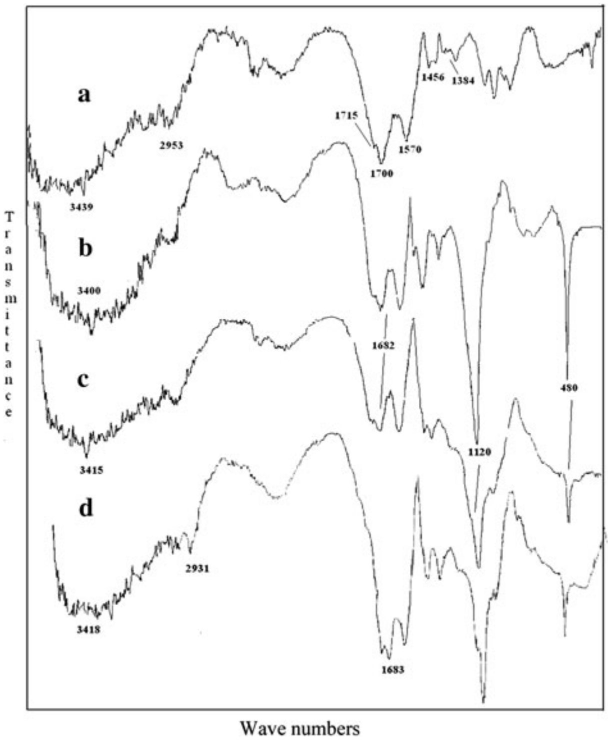

Fig. 1 FT-IR spectrum of poly(AAm-co-AAc) (**a**), poly(AAm-co-AAc)/clinoptilolite (**b**), poly(AAm-co-AAc)/NaY (**c**), and poly(AAm-co-AAc)/MCM-41 (**d**)

3,439 cm^{-1} is due to N–H groups of polyacrylamide and the peak at 1,700 cm^{-1} represents the carbonyl group. There is a shoulder at 1,715 cm^{-1} that corresponds to the carbonyl group of polyacrylate. Also we can see two bonds at 1,384 and 1,570 cm^{-1} related to COO^{-} group in polyacrylate and the peaks at 1,456 and 2,953 cm^{-1} represent the C–N and C–H bonding, respectively [23].

In (b), (c), and (d) spectrum, the peaks of carbonyl shifted to around 1,682 cm^{-1} and the intensity of the peaks at 3,400 cm^{-1} correspond to N–H decreased and shifted to lower frequency. It may be because of the formation of hydrogen bonding between COOH, NH_2 of the copolymer and hydroxyl groups of Al–OH and Si–OH in pore materials. In addition, we can see two bands at about 1,120 cm^{-1} due to Si–O and 480 cm^{-1} related to Al–OH in the composites.

XRD analysis

X-ray diffraction patterns of NaY, MCM-41 and clinoptilolite, poly(AAm-co-AAc)/NaY, poly(AAm-co-AAc)/clinoptilolite, and poly(AAm-co-AAc)/MCM-41 are shown in Fig. 2a–e, respectively. Some diffraction peaks at 2θ: 20°–80° are clearly

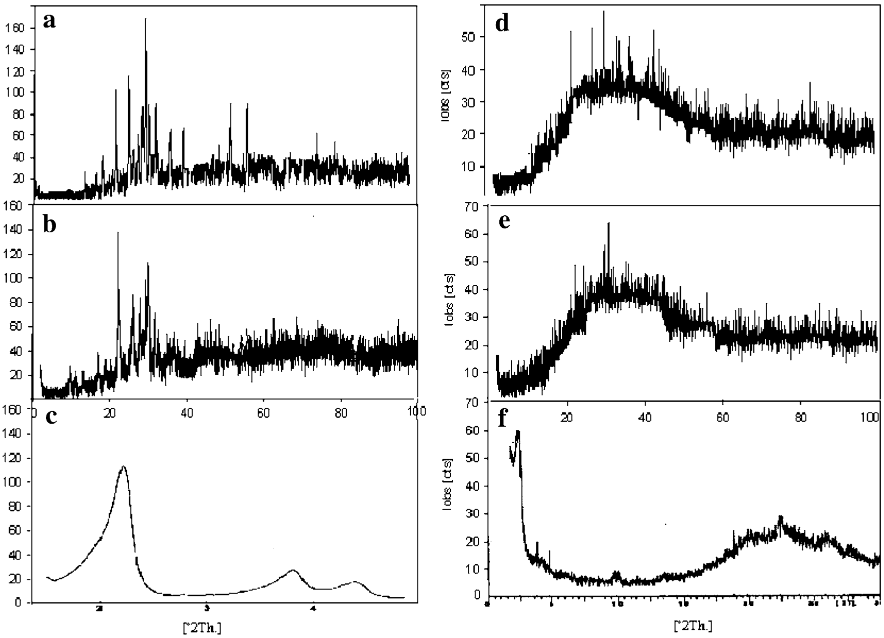

Fig. 2 X-ray diffraction patterns of NaY (**a**), clinoptilolite (**b**), MCM-41 (**c**), poly(AAm-co-AAc)/NaY zeolite (**d**), poly(AAm-co-AAc)/clinoptilolite (**e**), and poly(AAm-co-AAc)/MCM-41 (**f**)

seen and can be indexed as the NaY (Fig. 2c) and clinoptilolite (Fig. 2d) phase. Also, Fig. 2e shows some diffraction peaks at 2θ: 1°–5° are clearly seen and can be indexed as the MCM-41.

The wide peaks show that the size of NaY, MCM-41, and clinoptilolite particles is very small. The mean size of the particles is about 2 nm which is according to Scherr's equation [24]. In addition, decrease of intensity corresponds to covering particles with polymer. Hence, two broad peaks at 2θ: 12.3° and 20° can be observed are due to poly(AAm-co-AAc) [23].

TGA analysis

Figure 3a–d shows TGA thermograms of poly(AAm-co-AAc), poly(AAm-co-AAc)/NaY, poly(AAm-co-AAc)/clinoptilolite, and poly(AAm-co-AAc)/MCM-41, respectively. In Fig. 3a, degradation of polymeric network of poly(AAm-co-AAc) in a multi-step can be clearly seen, which is completed at temperature about 889 °C. Figure 1b, c, and d shows degradation of poly(AAm-co-AAc)/NaY, poly(AAm-co-AAc)/clinoptilolite, and poly(AAm-co-AAc)/MCM-41 completed at 958, 943, and 905 °C, respectively. These results show that the thermal stability of polymeric network increased with the addition of NaY, clinoptilolite, and MCM-41 nanoparticles [25]. It may be because of the formation of some bonds between COOH, NH_2 of the copolymer and hydroxyl groups of pore materials.

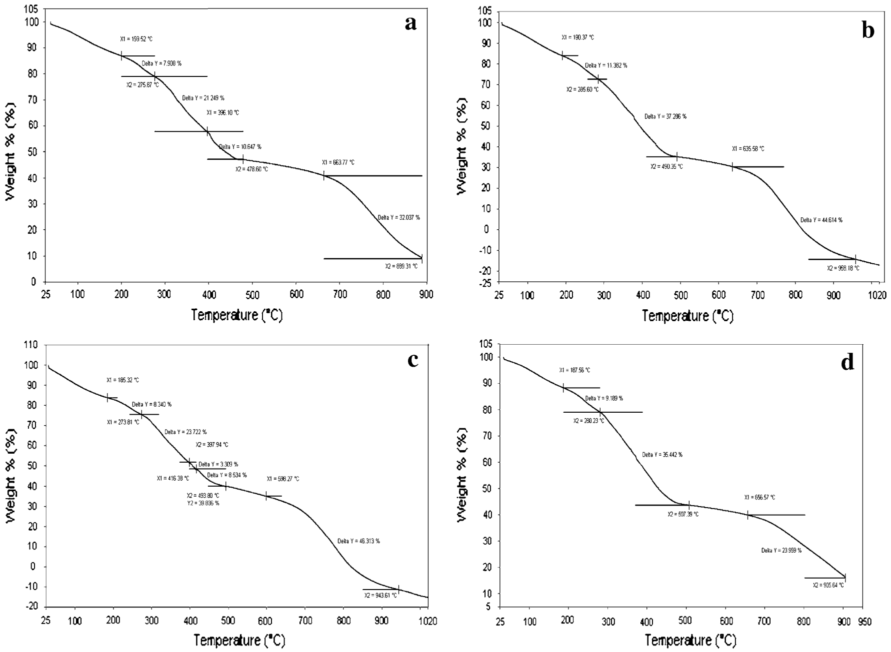

Fig. 3 TGA thermograms of poly(AAm-co-AAc) (**a**), poly(AAm-co-AAc)/NaY (**b**), poly(AAm-co-AAc)/clinoptilolite (**c**), and poly(AAm-co-AAc)/MCM-41 (**d**)

Morphology

SEM images of the NaY zeolite, clinoptilolite, MCM-41, poly(AAm-co-AAc)/NaY zeolite, poly(AAm-co-AAc)/clinoptilolite, and poly(AAm-co-AAc)/MCM-41 are shown in Fig. 4a–f, respectively. There is a considerable change between two samples. From the micrographs, it was found that the NaY, clinoptilolite, and MCM-41 were dispersed in the polymer network. Several areas show fine network structure. It means that NaY, clinoptilolite, and MCM-41 have good collaboration with poly(AAm-co-AAc) and improves the network of it, which may be favorable for cadmium and lead adsorption [26].

Adsorption study of lead and cadmium

The effect of contact time

Figure 5a, b shows the adsorption percentage of Lead and Cadmium versus time in the solution of Pb(II) and Cd(II) with 50 mg L^{-1} as initial concentration. The adsorption increases up to 120 min for Pb(II) and 60 min for Cd(II) and then saturated. Thus, it appears that time equilibrium of 120 and 60 min for Pb(II) and Cd(II) ions are required, respectively.

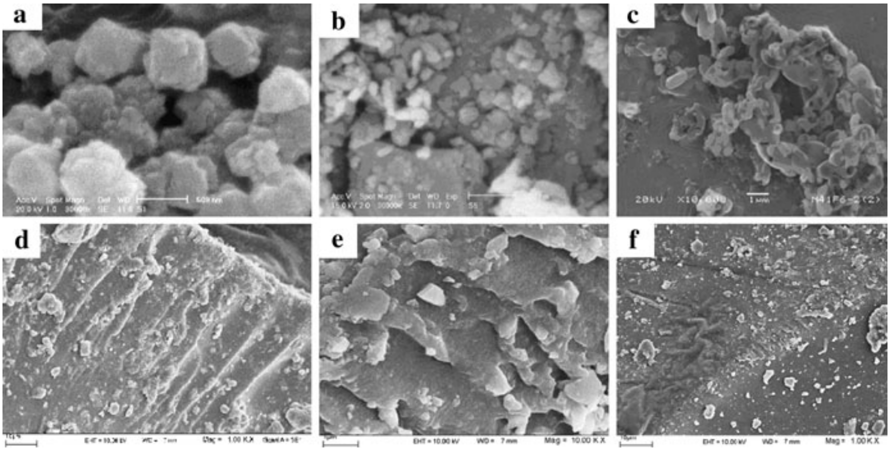

Fig. 4 SEM images of NaY (**a**), clinoptilolite (**b**), MCM-41 (**c**), poly(AAm-co-AAc)/NaY zeolite (**d**), poly(AAm-co-AAc)/clinoptilolite (**e**), and poly(AAm-co-AAc)/MCM-41 (**f**)

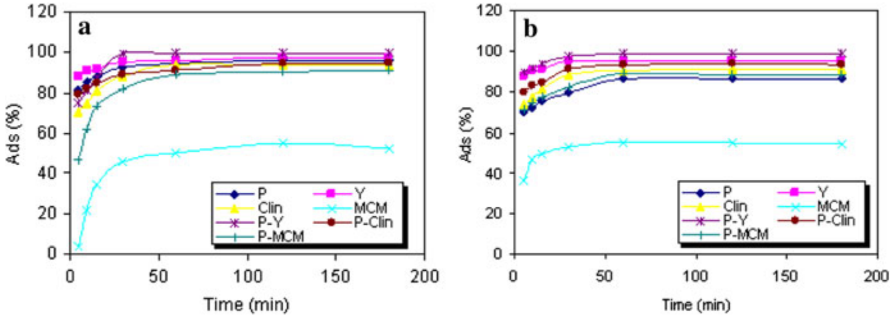

Fig. 5 Adsorption percent of Pb (**a**) and Cd (**b**) versus time by different composites with 25 mg of adsorbents in 50 mg L^{-1} solution of Pb and Cd at room temperature

The effect of initial concentration

Figure 6a, b shows the effect of initial concentration of heavy metal ions on the percentage adsorption. Results show that the amount of adsorption was significantly increased with initial heavy metal concentration especially in the case of Pb(II) and also for Cd(II) in the studied initial concentration range (50–500 mg L^{-1}). Also, we can see with increasing the initial concentration of Pb(II) and Cd(II) from 500 to 2,000 mg L^{-1} adsorption decreased due to saturation of the adsorption sites at the adsorbents. However, even in 2,000 mg L^{-1} of heavy metal ions the synthetic composites can be adsorbed about 60–83% of Pb(II) and 44–63% of Cd(II) in the solutions with different adsorbent.

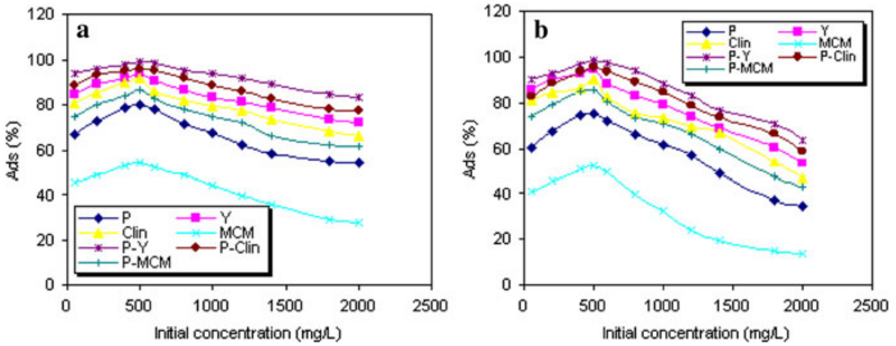

Fig. 6 Adsorption percent of Pb (**a**) and Cd (**b**) versus initial concentration by different composites with 25 mg of adsorbents in pH 5, 6 for Pb and Cd, respectively, at room temperature

Effect of pH on Pb(II) and Cd(II) adsorption

Figure 7a and b shows the effect of equilibrium pH on the amount of Pb(II) and Cd(II) adsorbed on various adsorbents. The adsorption removal of both metal ions strongly depends on solution pH. Results show that the adsorption capacity of heavy metal ions decreased at low pH. Also, the optimum pH for removal of Pb(II) and Cd(II) was determined about 5, 6, respectively. The pH of solution is one of the important factors in adsorption process. The smaller amount of metals adsorbed at low pH is probably due to competitive adsorption of H^+ with metal ions. These results confirmed that both the metal sites in the NaY zeolite and carboxylate groups in the poly(AAm-co-AAc) play a critical role for absorption metal ions [27–29].

Effect of adsorbent content

Figure 8a, b shows the percentage adsorption of Lead and Cadmium at different content of adsorbent. The results show that with increasing of adsorbent content from 5 to 25 mg for 25 mL Cd(II) and Pb(II) solution (50 mg L^{-1}) at optimum pH, time, and temperature, the removal of Cd(II) and Pb(II) increased. In addition,

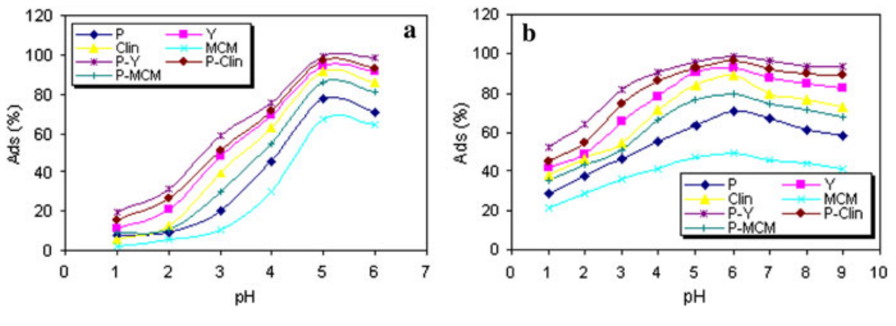

Fig. 7 Adsorption percent of Pb (**a**) and Cd (**b**) versus pH by different composites with 25 mg of adsorbents in 50 mg L^{-1} solution of Pb and Cd at room temperature

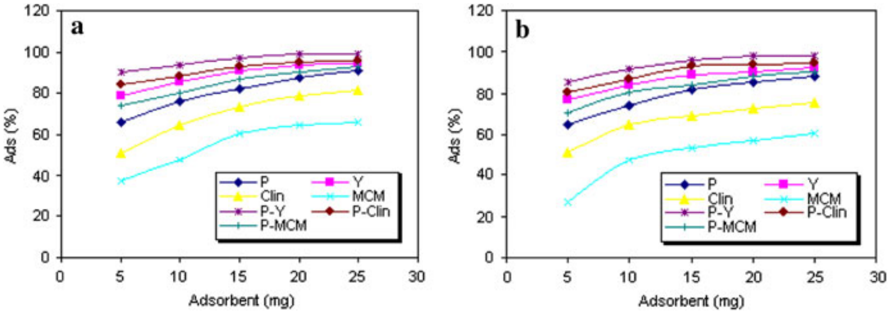

Fig. 8 Adsorption percent of Pb (**a**) and Cd (**b**) versus adsorbent content by different composites in 50 mg L^{-1} solution of Pb and Cd and pH 5, 6 for Pb and Cd, respectively, at room temperature

further increasing the adsorbent content had negligible effect on the adsorption of metals. Literature review shows that the content of our adsorbent was less than adsorbents' content in many other works and it can be economical [6, 18, 30].

Effect of temperature

Figure 9a, b shows the effect of temperature in the range of 283–323 K on the adsorption of heavy metals on the various absorbent. We can see with increasing of temperature until 303 K the adsorption of heavy metals increased. Then, the adsorption process has endothermic nature. In addition, with increasing temperature up to 323 K adsorption of heavy metals decreased that may be due to some desorption of heavy metals [6].

Comparison between the poly(AAm-co-AAc)/NaY zeolite, poly(AAm-co-AAc)/MCM-41, and poly(AAm-co-AAc)/clinoptilolite

Figures 10 and 11 show that NaY zeolite has higher adsorption behavior related to clinoptilolite and MCM-41. This can be explained by ability of porous material in ion-exchange interaction. It seems, NaY zeolite with Na_{56} (Al_{56} Si_{136} O_{384}) formula and by almost spherical cages (12A° of diameter) tetrahedral interconnected through smaller windows (7.4A° of diameter) defined by 12 oxygen rings is a good adsorbent for Pb(II) and Cd(II) related to clinoptilolite with (Ca_4 Mg_{18} Na_4 K_{28}) ($Al_{8.16}$ $Si_{27.84}$ O_{72}) $(H_2O)_{25.52}$ formula by smaller channel. Furthermore, there are no any cation sites in the MCM-41 for that exchange with Pb(II) and Cd(II) and there are only interaction between Si–O$^-$ in calcinated MCM-41 and metal cations. Nevertheless, results show that the adsorption ability of NaY zeolite, MCM-41, and clinoptilolite increased with added poly(AAm-co-AAc). It seems, carboxylic groups of the copolymer are good sites for trapping the Pb(II) and Cd(II). These data indicate that the poly(AAm-co-AAc)/NaY, poly(AAm-co-AAc)/MCM-41, and poly(AAm-co-AAc)/clinoptilolite exhibit superior Pb(II) (about 90–99%) and Cd(II) (about 88–98%) adsorption behavior. It is because there are a lot of charges on the NaY zeolite, MCM-41, clinoptilolite, and poly(AAm-co-AAc) which

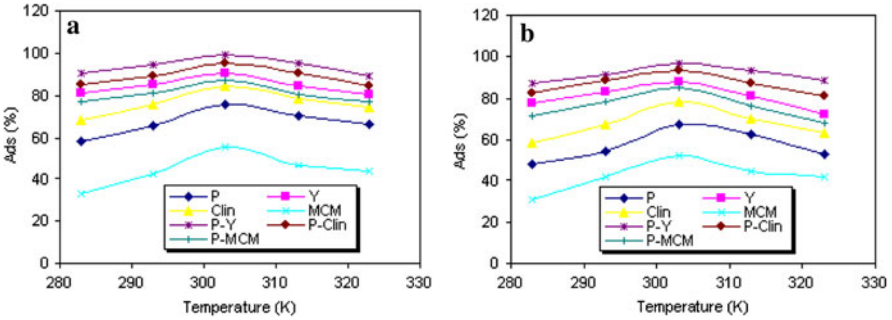

Fig. 9 Adsorption percent of Pb (**a**) and Cd (**b**) versus temperature by different composites with 25 mg of adsorbents in 50 mg L^{-1} solution of Pb and Cd and pH 5, 6 for Pb and Cd, respectively

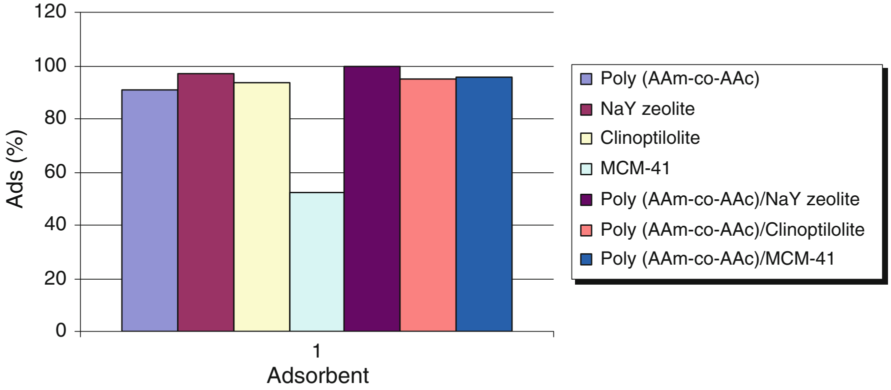

Fig. 10 Comparison between different adsorbents in adsorption of Pb(II)

adsorbed Pb(II) and Cd(II) (Fig. 12). Therefore, the composites have good porosity and flexibility for metal ions that can be introduced into network easily and interacted with NaY, MCM-41, clinoptilolite, and poly(AAm-co-AAc).

Desorption study

The prepared composite materials should be making the adsorbent economically complete. As mentioned, the poly(AAm-co-AAc)/NaY nanocomposite had the best adsorption behavior of Pb(II) and Cd(II). Therefore, we selected it to desorption study. It was investigated that this nanocomposite could adsorb about 99% of the Pb(II) and Cd(II). Therefore, in the first cycle, it was treated with 0.01 N H_2SO_4 and stirred for 1 h. Then, it was shown 96% of Pb(II) and 94% of Cd(II) desorption. Adsorbed Pb(II) and Cd(II)could be stripped in 1 h by the introduction of protons that competed with metal ions for binding sites. In the next step from this cycle, the same poly(AAm-co-AAc)/NaY nanocomposite could remove 95% Pb(II) and 92% Cd(II).

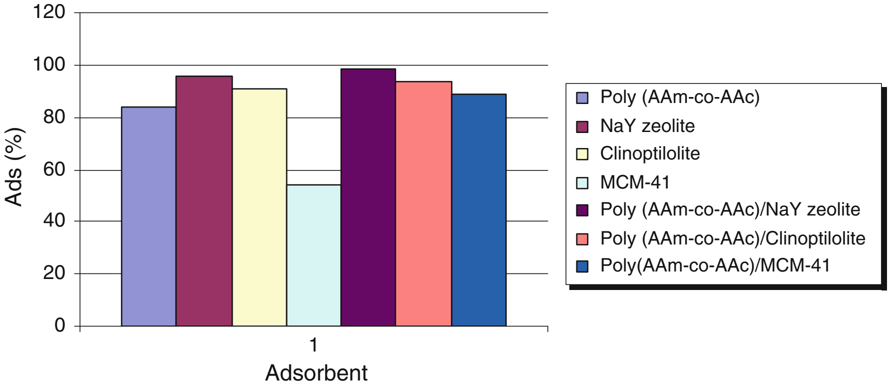

Fig. 11 Comparison between different adsorbents in adsorption of Cd(II)

It is presented in Fig. 13 that the removal effect decreased per cycle but even in the 10th cycle the adsorbent could remove 60% Pb and 54% Cd ions, which could be desorbed to 46% Pb(II) and 39% Cd(II). Hence, it appeared that during desorption just the metal ions which were adsorbed by physical forces get desorbed.

Adsorption isotherm studies

Adsorption isotherm studied by fitted data to the Langmuir and Freundlich isotherms that show have monolayer or multilayer sorption [31]. The Langmuir isotherm is valid for monolayer sorption due to a surface of a finite number of identical sites and expressed in the linear form as Eq. 2

$$C_e/q_e = 1/bq_{\max} + C_e/q_{\max} \tag{2}$$

where C_e is the equilibrium concentration (mg L^{-1}) and q_e is the amount of adsorbed ion at equilibrium (mg g^{-1}). The Langmuir constant $q_{\max}$ (mg g^{-1}) represent the monolayer adsorption capacity and b (L mg^{-1}) relates to the heat of adsorption. The Langmuir isotherm plots for adsorption of Pb(II) and Cd(II) on the various absorbent from aqueous solutions are shown in Figs. 14 and 15, respectively.

The essential feature of the Langmuir adsorption can be expressed by R_L factor. A dimensionless constant referred to as separation factor or equilibrium parameter for predicting whether an adsorption system is favorable or unfavorable. Also, R_L is calculated by using the Eq. 3

$$R_L = 1/1 + bC_o \tag{3}$$

where b is the Langmuir constant and C_o is the initial heavy metal ions concentration (mg L^{-1}) which if R_L values are between 0 and 1, the adsorption is favorable [32]. For all of the synthesized nanocomposites, R_L was calculated between 0 and 1, thus adsorption by them is favorable.

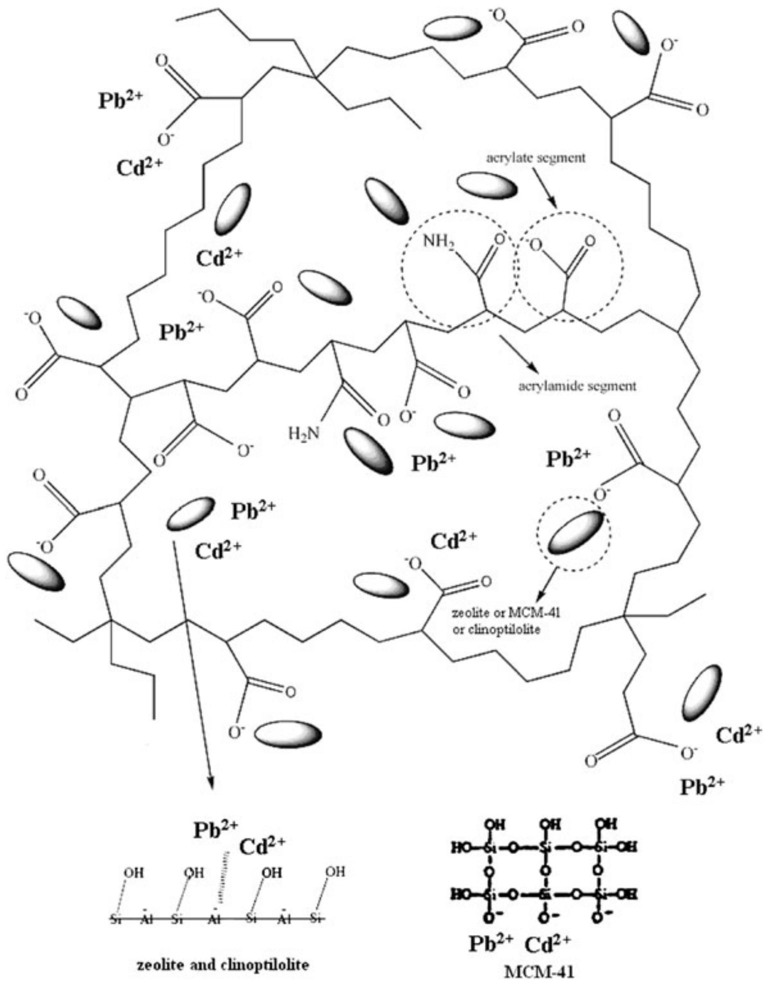

Fig. 12 Schematic representation of formation of ionic interaction between metal ions and the carboxylic group in polymer network and the surface of zeolite, MCM-41, and clinoptilolite

The Freundlich isotherm describes the heterogeneous surface energies by multilayer adsorption and is expressed in linear form as Eq. 4

$$\ln q_e = \ln K_f + 1/n \ln C_e \tag{4}$$

where K_f indicates adsorption capacity (mg g^{-1}) and n is an empirical parameter related to the intensity of adsorption, which varies with the heterogeneity of the adsorbent. The Freundlich isotherm plots for the adsorption of Pb(II) and Cd(II) on synthetic materials in aqueous solutions are shown in Figs. 16 and 17, respectively.

The equilibrium data fitted to Langmuir model better than Freundlich model indicating monolayer adsorption. The values of Langmuir and Freundlich constants are presented in Tables 1 and 2.

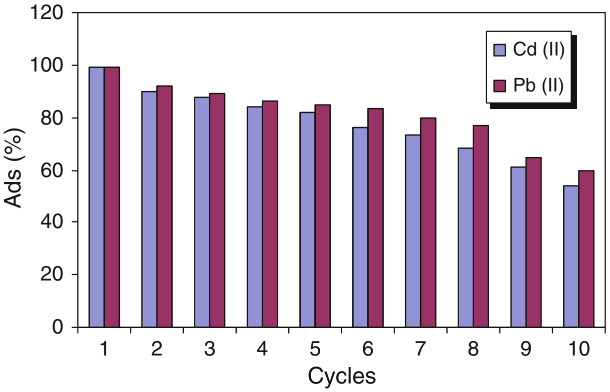

Fig. 13 Desorption study of Cd(II) and Pb(II) by poly(AAm-co-AAc)/NaY with the optimized conditions

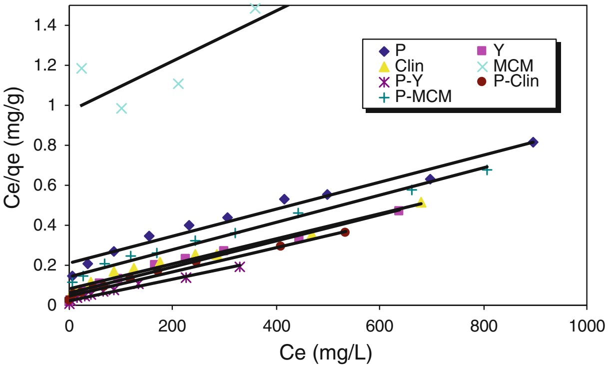

Fig. 14 Langmuir isotherm plots for the adsorption of Pb(II) on synthetic materials in aqueous solutions at pH 5

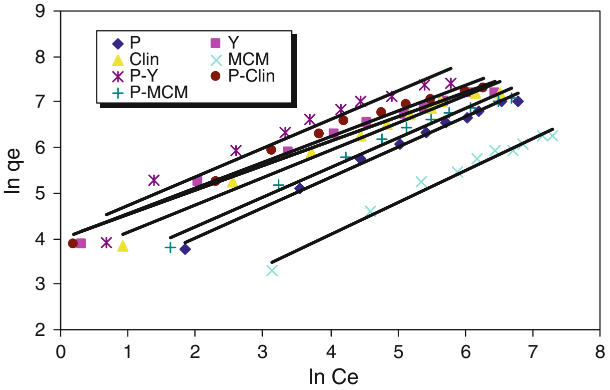

Fig. 15 Freundlich isotherm plots for the adsorption of Pb(II) on synthetic materials in aqueous solutions at pH 5

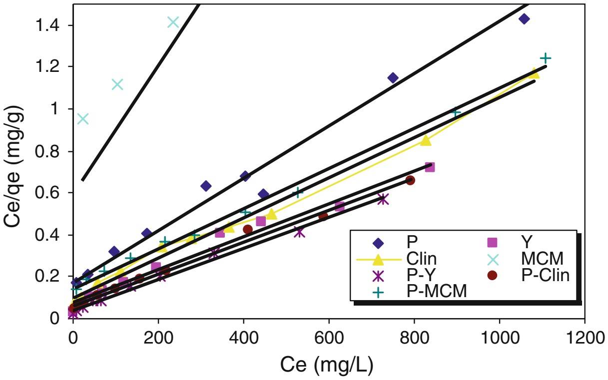

Fig. 16 Langmuir isotherm plots for the adsorption of Cd(II) on synthetic materials in aqueous solutions at pH 6

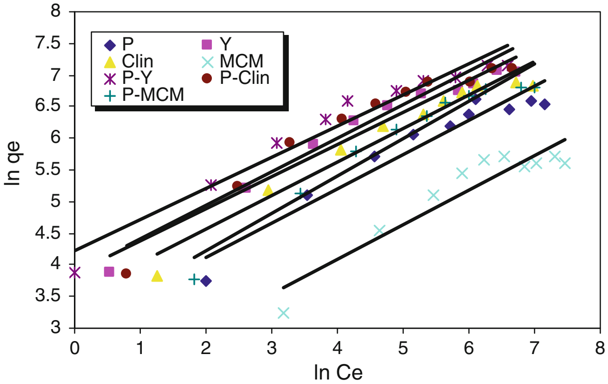

Fig. 17 Freundlich isotherm plots for the adsorption of Cd(II) on synthetic materials in aqueous solutions at pH 6

Table 1 Langmuir and Frundlich constant for the adsorption of Pb(II)

Adsorbent	Langmuir isotherm			Freundlich isotherm		
	q_{max} (mg g^{-1})	b (L mg^{-1})	R^2	n	K_f (mg g^{-1})	R^2
Poly(AAm-co-AAc)	1428.57	0.003	0.9676	1.51	14.77	0.9907
Zeolite Y	1428.57	0.012	0.9704	1.86	53.76	0.9792
Clinoptilolite	1666.66	0.007	0.9738	1.65	34	0.9813
MCM-41	769.23	0.001	0.9642	1.42	3.67	0.9789
P-Zeolite Y	2,000	0.018	0.9798	1.58	59.48	0.9322
P-Clin	1666.66	0.001	0.9879	1.77	54.07	0.9785
P-MCM	1428.57	0.005	0.9906	1.54	19.52	0.9791

Table 2 Langmuir and Frundlich constant for the adsorption of Cd(II)

Adsorbent	Langmuir isotherm			Freundlich isotherm		
	$q_{\max}$ (mg g^{-1})	b (L mg^{-1})	R^2	n	K_f (mgg^{-1})	R^2
Poly(AAm-co-AAc)	833.33	0.040	0.9907	1.86	21.15	0.9276
Zeolite Y	1,000	0.100	0.9909	1.96	47.77	0.9652
Clinoptilolite	1,250	0.106	0.9828	1.89	33.27	0.9509
MCM-41	322.58	0.005	0.9791	1.81	6.52	0.8746
P-Zeolite Y	1428.57	0.016	0.9945	2.03	68.54	0.9511
P-Clin	1,250	0.013	0.9925	1.88	48.26	0.9342
P-MCM	1,000	0.007	0.9950	1.70	21.22	0.9440

Table 3 Removal capacities of Pb(II) by various adsorbents

Adsorbent	$q_{\max}$ (mgg^{-1})	References
Activated carbon	31.2	Machida et al. [33]
Crop milling waste	49.97	Saeed et al. [34]
PHEMA/chitosan membranes	68.81	Genc et al. [35]
Wheat bran	87	Bulut et al. [36]
Palm shell activated carbon	95.2	Issabayeva et al. [37]
Natural phosphate	115.3	Mouflih et al. [38]
Activated phosphate	155	Mouflih et al. [38]
HAp/PAAm gel	178	Hyun Jang et al. [39]
Synthesized composites	**769–2000**	This work

As shown in Table 3 different adsorbents have been compared regarding to Pb ions' removal capacity. The $q_{\max}$ of synthesized nanocomposite in current study is significantly higher than other reported adsorbents. Also, the removal capacity of synthesized nanocomposite and other adsorbent in adsorption of Cd(II) is shown in Table 4 that $q_{\max}$ of the nanocomposite we prepared is comparable with the reported adsorbents.

Conclusion

The poly acrylamide-co-acrylic acid/NaY zeolite, poly acrylamide-co-acrylic acid/MCM-41, and poly acrylamide-co-acrylic acid]/clinoptilolite composites were synthesized and the removal effect of Pb(II) and Cd(II) was determined in them. Results show that the adsorption increases up to 120 min for Pb(II) and 60 min for Cd(II). The studied temperature was in the range of 283–323 K and adsorption process is endothermic process. Also, the poly(AAm-co-AAc)/NaY nanocomposite had the best adsorption behavior of Pb(II) and Cd(II) about 99%. Desorption study shows that even after 10 cycle have a good adsorption behavior for metal ions. Finally, the equilibrium removal performance of the composites is analyzed

Table 4 Removal capacities of Cd(II) by various adsorbents

Adsorbent	$q_{\max}$ (mg g^{-1})	References
Aerobic granules	172.7	Liu et al. [40]
Dithiocarbamate-anchored polymer/organosmectite	82.2	Say et al. [41]
Silicagel bonded by 1,5-diphenylcarbazone	0.44	Fan et al. [42]
Biomatrix from rice husk	16.74	Krishnani et al. [43]
Sol–gel silica doped with 1-(2-pyridylazo)-2-naphthol	0.49	Khan et al. [44]
Calotropis procera	50.5	Pandey et al. [45]
Guar-graft-poly(acrylamide) silica composite	2,000	Singh et al. [6]
Synthesized composites	**322–1428**	This work

according to the Langmuir and Freundlich adsorption isotherm model that shows results fitted to Langmuir model and have monolayer adsorption.

References

1. Sayari A, Hamoudi S, Yang Y (2005) Application of pore-expanded mesoporous silica. 1. Removal of heavy metal cations and organic pollutants from wastewater. Chem Mater 17:212–216
2. Ma QY, Traina SJ, Ryan JA (1994) Effects of aqueous Al, Cd, Cu, Fe(II), Ni and Zn on Pb immobilization by hydroxyapatite. Environ Sci Technol 28:1219–1228
3. Brigatti MF, Medici L, Poppi L (1996) Sepiolite and industrial waste-water purification: removal of Zn^{2+} and Pb^{2+} from aqueous solutions. Appl Clay Sci 11:45–54
4. Prasad M, Saxena S, Amritphale SS, Chandra N (2000) Kinetics and isotherms for aqueous lead adsorption by natural minerals. Ind Eng Chem Res 39:3034–3037
5. Organisation for Economic Co-operation and Development (OECD) (1994) Risk Reduction Monograph No. 5: Cadmium OECD Environment Directorate, Paris, France
6. Singh V, Pandey S, Singh SK, Sanghi R (2009) Removal of cadmium from aqueous solutions by adsorption using poly(acrylamide) modified guar gum-silica nanocomposites. Sep Purif Technol 67:251–261
7. Waalkes MP (2000) Cadmium carcinogenesis in review, review. J Inorg Biochem 79:241–244
8. Radhika V, Subramanian S, Natarajan KA (2006) Bioremediation of zinc using *Desulfotomaculum nigrificans*: bioprecipitation and characterization studies. Water Res 40:3628–3636
9. Celis R, Hermosin MC, Cornjo J (2000) Heavy metal adsorption by functionalized clays. Environ Sci Technol 34:4593–4599
10. Ginzburg VV, Singh C, Balazs AC (2000) Theoretical phase diagrams of polymer/clay composites: the role of grafted organic modifiers. Macromolecules 33:1089–1099
11. Lagadic IL, Mitchell MK, Payne BD (2001) Highly effective adsorption of heavy metal ions by thiol-functionalised magnesium phyllosilicate clay. Environ Sci Technol 35:984–990
12. Kasgoz H, Durmus A, Kasgoz A (2008) Enhanced swelling and adsorption properties of AAm-AMPSNa/clay hydrogel nanocomposites for heavy metal ion removal. Polym Adv Technol 19:213–220
13. Lee WF, Yang LG (2004) Super absorbent polymeric materials. XII. Effect of montmorillonite on water absorbency for poly (sodium acrylate) and montmorillonite nanocomposite super absorbents. J Appl Polym Sci 92:3422–3429
14. Zhang JP, Li A, Wang AQ (2006) Superabsorbent composite. X. Effects of saponification on properties of polyacrylamide/attapulgite. Polym Eng Sci 46:1762–1767
15. Wu JH, Wei YL, Lin JM, Lin SB (2003) Study on starch–graft-acrylamide/mineral powder superabsorbent composite. Polymer 44:6513–6520

16. Lee WF, Chen YC (2005) Effect of intercalated reactive mica on water absorbency for poly (sodium acrylate) composite superabsorbent. Eur Polym J 41:1605–1612
17. Alhakawati MS, Banks CJ (2004) Removal of copper from aqueous solution by *Ascophyllum nodosum* immobilized in hydrophilic polyurethane foam. J Environ Manag 72:195–204
18. Ulusoy U, Simsek S (2005) Lead removal by polyacrylamide-bentonite and zeolite composites: effect of phytic acid immobilization. J Hazard Mater 127:163–171
19. Pinto ML, Pires J, Carvalho AP, de Carvalho MB, Bordado JC (2006) Synthesis and regeneration of polyurethane/adsorbent composites and their characterization by adsorption methods. Microporous Mesoporous Mater 89:260–269
20. Breck DW, Tonawanda NY (1964) Assigned to Union Carbide, Pat. no. 3130007, Patented Appr., 21
21. Tanev PT, Pinnavaia TJ (1996) Mesoporous silica molecular sieves prepared by ionic and neutral surfactant templating: a comparison of physical properties. Chem Mater 8:2068–2079
22. Zendehdel M, Barati A, Alikhani H, Hekmat A (2009) Removal of methylene blue dye from wastewaters by absorption on to sIPN hydrogels composed of poly(Acrylamide-co-Acrylicacid) and poly vinyl alcohol. In: 1st International conference on advances in wastewater treatment and reuse, 10–12 November 2009, Tehran, Iran
23. Ni Y-H, Ge X-W, Zhang Z-C (2005) Preparation and characterization of ZnS/poly (AAm-co-AAc) dendritically nanocomposites by γ-irradiation. Mater Sci Eng 119:51–54
24. Klug HP, Leroy EA (1974) X-ray diffraction procedure. Wiley, New York, p 354
25. Lin R, Chen B, Chen G, Wu J, Chiu H, Suen Sh (2009) Preparation of porous PMMA/Na+-montmorillonite cation-exchange membranes for cationic dye adsorption. J Membr Sci 326:117–129
26. Yi JZ, Zhang LM (2008) Removal of methylene blue dye from aqueous solution by adsorption onto sodium humate/polyacrylamide/clay hybrid hydrogels. Bioresour Technol 99:2182–2186
27. Quintelas C, Rocha Z, Silva B, Fonseca B, Figueiredo H, Tavares T (2009) Removal of Cd(II), Cr(VI), Fe(III) and Ni(II) from aqueous solutions by an *E. coli* biofilm supported on kaolin. Chem Eng J 149:319–324
28. Asçi Y, Nurbas M, Sag Açikel Y (2007) Sorption of Cd(II) onto kaolin as a soil component and desorption of Cd(II) from kaolin using rhamnolipid biosurfactant. J Hazard Mater B 139:50–56
29. Rangsayatorn N, Pokethitiyook P, Upatham ES, Lanza GR (2004) Cadmium biosorption by cells of *Spirulina platensis* TISTR 8217 immobilized in alginate and silica gel. Environ Int 30:57–63
30. Harahsheh M, Shawabkeh R, Al-Harahsheh A, Tarawneh Kh, Batiha MM (2009) Surface modification and characterization of *Jordanian kaolinite*: application for lead removal from aqueous solutions. Appl Surf Sci 255:8098–8103
31. Basha S, Murthy VP (2006) Seaweeds for engineering metal biosorption: a review. In: Mason LG (ed) Mason in focus on hazardous materials research, 1st edn. Nova Science Publishers, New York, p 182
32. Singh KK, Talat M, Hasan SH (2006) Removal of lead from aqueous solutions by agricultural waste maize bran. Bioresour Technol 97:2124–2130
33. Machida M, Yamazaki R, Aikawa M, Tatsumoto H (2005) Role of minerals in carbonaceous adsorbents for removal of Pb(II) ions from aqueous solution. Sep Purif Technol 46:88–94
34. Saeed A, Iqbal M, Akhtar MW (2005) Removal and recovery of lead(II) from single and multimetal (Cd, Cu, Ni, Zn) solutions by crop milling waste (black gram husk). J Hazard Mater 117:65–73
35. Genc O, Soysal L, Bayramoglu G, Arica MY, Bektas S (2003) Procion Green H-4G immobilized poly(hydroxyethylmethacrylate/chitosan)compositemembranes for heavy metal removal. J Hazard Mater 97:111–125
36. Bulut Y, Baysal Z (2006) Removal of Pb(II) from wastewater using wheat bran. J Environ Manag 78:107–113
37. Issabayeva G, Aroua MK, Sulaiman NMN (2006) Removal of lead from aqueous solutions on palm shell activated carbon. Bioresour Technol 97:2350–2355
38. Mouflih M, Aklil A, Sebti S (2005) Removal of lead from aqueous solutions by activated phosphate. J Hazard Mater 119:183–188
39. Jang SH, Jeong YG, Min BG, Lyoo WS, Lee S Ch (2008) Preparation and lead ion removal property of hydroxyapatite/polyacrylamide composite hydrogels. J Hazard Mater 159:294–299
40. Liu Y, Xu H, Yang S-F, Tay J-H (2003) A general model for biosorption of Cd^{2+}, Cu^{2+} and Zn^{2+} by aerobic granules. J Biotechnol 102:233–239
41. Say R, Birlik E, Denizli A, Ersoz A (2006) Removal of heavy metal ions by dithiocarbamate-anchored polymer/organosmectite composites. Appl Clay Sci 31:298–305

42. Fan J, Qin Y, Feng S, Hu Z (2005) Preparation and application of silica gel bonded by 1,5-diphenylcarbazone for enrichment and separation of heavy metal ions from water. Fenxi Huaxue 33: 1151–1154
43. Krishnani KK, Meng X, Christodoulatos C, Boddu VM (2008) Biosorption mechanism of nine different heavy metals onto biomatrix from rice husk. J Hazard Mater 153:1222–1234
44. Khan A, Mahmood F, Ahmed S, Khokhar MY (2003) Removal of Cd ions by sol–gel silica dopedwith 1-(2-pyridylazo)-2-naphthol. J Sol Gel Sci Technol 27:221–224
45. Pandey PK, Verma Y, Choubey S, Pandey M, Chandrasekhar K (2008) Biosorptive removal of cadmium from contaminated groundwater and industrial effluents. Bioresour Technol 99:4420–4427